

Structure based mechanism of the Ca^{2+} -induced release of coelenterazine from the *Renilla* binding protein

Galina A. Stepanyuk,^{1,2} Zhi-Jie Liu,^{3*} Eugene S. Vysotski,^{2,1} John Lee,¹ John P. Rose,¹ and Bi-Cheng Wang¹

¹ Department of Biochemistry and Molecular Biology, University of Georgia, Athens, Georgia 30602

² Photobiology Laboratory, Institute of Biophysics, Russian Academy of Sciences Siberian Branch, Krasnoyarsk 660036, Russia

³ National Laboratory of Biomacromolecules, Institute of Biophysics, Chinese Academy of Sciences, 15 Datun Road, Beijing 100101, People's Republic of China

ABSTRACT

The crystal structure of the Ca^{2+} -loaded coelenterazine-binding protein from *Renilla muelleri* in its apo-state has been determined at resolution 1.8 Å. Although calcium binding hardly affects the compact scaffold and overall fold of the structure before calcium addition, there are easily discerned shifts in the residues that were interacting with the coelenterazine and a repositioning of helices, to expose a cavity to the external solvent. Altogether these changes offer a straightforward explanation for how following the addition of Ca^{2+} , the coelenterazine could escape and become available for bioluminescence on *Renilla* luciferase. A docking computation supports the possibility of a luciferase-binding protein complex.

Proteins 2009; 74:583–593.
© 2008 Wiley-Liss, Inc.

Key words: bioluminescence; EF-hand; coelenteramide; luciferase; Ca^{2+} -binding protein.

INTRODUCTION

Renilla luciferase is a bioluminescent protein that has found wide application, as a gene probe, for *in vivo* imaging, in diagnostic kits, and in other areas of biological research and biomedicine.¹ The popularity of such bioluminescence systems as probes results from the fact that the light emission and therefore the subject of the analysis, can be detected with extreme sensitivity.

Renilla luciferase catalyzes the molecular oxygen addition to coelenterazine, an imidazopyrazinone derivative, followed by its oxidative decarboxylation, to populate the product coelenteramide in its first electronic excited state. The blue bioluminescence, a broad band with maximum at 480 nm, originates from this fluorescence state of the coelenteramide. *Renilla* luciferase was first isolated from the Sea Pansy, *Renilla reniformis*, a soft coral found in shallow water marine environments.² The bioluminescence property probably functions to deter predators from nibbling at the polyps. Besides luciferase, the *in vivo* bioluminescence system localized within the photophore, involves two other proteins, the *Renilla* green-fluorescent protein, which modulates the color of the light emission, and a Ca^{2+} -triggered coelenterazine-binding protein (CBP).^{3,4} The CBP is the same as the luciferin-binding protein (LBP) described by Charbonneau and Cormier.³ When this protein was isolated from *R. reniformis* they called it “luciferin-binding protein” because the chemical structure of the *Renilla* luciferin had not been established at that time. As the chemical identification of the luciferin is now well established and to avoid confusion with unrelated luciferin-binding proteins such as the one involved in dinoflagellate bioluminescence,⁵ we prefer “coelenterazine” as a rational replacement of the generic term “luciferin”, that is the specific name “coelenterazine-binding protein”. On disturbing the *Renilla*, the animal's nerve net induces a calcium ion flux setting off the bioluminescent flash over a time scale of tens of milliseconds. The role of CBP in this process evidently is 2-fold. As coelenterazine is unstable in free solution and as the membrane permeability of coelenterazine is rather high, these loss processes are prevented from occurring. CBP is an EF-hand protein^{6,7} and its calcium binding property therefore provides the animal the ability to sense the presence of

Grant sponsor: National Institutes of Health; Grant number: 1P50 GM62407; Grant sponsor: National Natural Science Foundation of China; Grant number: 30670427; Grant sponsor: Ministry of Science and Technology of China; Grant numbers: 2006AA02A316, 2006CB910901; Grant sponsor: Russian Foundation for Basic Research; Grant number: 05-04-48271; Grant sponsor: Russian Academy of Sciences; Grant sponsor: CAS Research Grant; Grant number: 07CF09; Grant sponsor: Bureau of International Cooperation, CAS (China-Russia Joint Research Grant); Grant sponsor: U. S. Department of Energy; Grant number: W-31-109-Eng-38.

*Correspondence to: Zhi-Jie Liu, National Lab of Biomacromolecules, Institute of Biophysics, Chinese Academy of Sciences, 15 Datun Road, Beijing 100101, People's Republic of China. E-mail: zjliu@ibp.ac.cn

Received 24 January 2008; Revised 5 May 2008; Accepted 2 June 2008

Published online 24 July 2008 in Wiley InterScience (www.interscience.wiley.com). DOI: 10.1002/prot.22173

danger. On binding Ca^{2+} , the coelenterazine becomes available as a substrate for the luciferase and the bioluminescent flash response occurs. Possibly this reaction occurs in a luciferase-CBP complex so that the coelenterazine does not necessarily dissociate completely and be exposed to autooxidation in free solution.⁷

It is the purpose of our structure determinations to account for these properties of CBP. This work presents the structure of the apo-CBP with a Ca^{2+} loaded into each of the three consensus loops. The coelenterazine is not present in the binding cavity. By comparison with the CBP structure bound with coelenterazine⁸ the mechanism of dissociation becomes apparent. On ligation of Ca^{2+} , shifts of certain helices create a “hole” thereby increasing the exposure of the binding cavity to solvent. Furthermore, residues in the binding cavity that were interacting with the coelenterazine are repositioned so that it becomes impossible for the coelenterazine to continue interacting simultaneously with all these original residues, thus weakening the affinity and allowing the molecule to protrude or escape through the opened hole. This conclusion is also supported by molecular docking of luciferase and apo-CBP loaded with Ca^{2+} according to which the “opened hole” in CBP lies opposite the putative *Renilla* luciferase active site.

METHODS

Cloning cDNA encoding CBP, expression in *E. coli* cells, and protein purification

The cloning and expression procedures have already been reported.⁷ Briefly, the poly(A)+RNA was isolated from ~20 tentacles of three live specimens using the Straight A's mRNA Isolation System (Novagen). Clontech's SMART cDNA Library Construction Kit was used to synthesize the double strand (ds) cDNA from the poly(A)+RNA sample. The fragment of cDNA encoding CBP was obtained by performing PCR with degenerate primers. These primers were designed using the published amino acid sequence for CBP from *R. reniformis*.⁶ Several isolated clones contained the 5'-ends of the CBP cDNA genes. From alignment of these isolated 5'-sequences the new primer complementary to the 5'-end of the CBP cDNA was designed and the full size cDNA gene for *R. muelleri* CBP cloned by PCR. For the bacterial expression of CBP, the coding sequence was amplified using specific primers and cloned for expression in a pET-19b vector (Novagen).

To produce protein for the structure determination of Ca^{2+} -loaded apo-CBP, the transformed *E. coli* cells (strain BL21-CodonPlus (DE3)-RIL (Novagen)) were cultivated with vigorous shaking in LB medium containing 200 $\mu\text{g mL}^{-1}$ ampicillin at 37°C and induced with 1 mM IPTG when the culture reached an OD_{590} of 0.7–0.8. After induction the cultivation was continued for 3 h.

Table I

Summary of Crystallographic Statistics

Statistics	Refinement data	Phasing data
Data processing		
Resolution range (Å)	50.00–1.8 (10.00–1.8)	50.00–2.45 (2.54–2.45)
Wavelength (Å)	1.0	1.7
Space group	P 6 ₅	P 6 ₅
Cell dimensions (Å)	$a = b = 78.41,$ $c = 125.00$	$a = b = 78.41,$ $c = 125.00$
Unique reflections (free)	37,300 (2079)	29721 (1489)
Completeness (%)	100	98.57
$I/\sigma(I)$	38.77 (2.25)	39.5 (3.05)
R_{sym} (%)	15 (32)	7 (33.0)
Redundancy	6.7 (2.7)	13 (2.4)
Refinement		
No. of molecules/A.U.	2	2
Resolution range (Å)	10.00–1.8	10.00–1.72
R_{work} (R_{free})	20.00 % (25.00%)	19.88 % (22.89%)
Mean B factor (Å ²)	21.749	18.61
Protein atoms (solvent)	2798 (300)	1498 (188)
RMSD bond lengths (Å)	0.016	0.018
RMSD bond angles (°)	1.459	1.314

Protein purification

Most of the apo-CBP produced in the *E. coli* accumulates in inclusion bodies that can be easily isolated by centrifugation. The purification was performed as previously reported for recombinant obelin.⁹ The apo-CBP sample in 6M urea obtained after chromatography on DEAE Sepharose Fast Flow was refolded by a 10-fold dilution in 20 mM Tris-HCl pH 7.1 with 1 mM CaCl_2 and purified by ion-exchange chromatography on DEAE-10 (Bio-Rad). Then the Ca^{2+} -loaded apo-CBP was concentrated and the chromatography buffer was replaced by 1 mM calcium acetate, 10 mM Bis-Tris pH 6.5. The protein concentration for crystallization was 13.5 mg mL^{-1} (Bio-Rad assay).

Crystallography

Initial screening for crystallization was carried out under 384 commercial conditions and by other methods described elsewhere.¹⁰ The crystals of Ca^{2+} -loaded apo-CBP were grown from 0.1M HEPES pH 7.5, 2% PEG 400, 2.0M ammonium sulfate over less than 5 days incubation at 4°C. The crystals were frozen in liquid nitrogen in a cryoprotectant solution of 4.0M Li_2SO_4 . The diffraction data were collected at 1.7 Å for phasing and 1.0 Å for refinement separately at beamline 22ID of the Advanced Photon Source. A continuous sweep of 360 consecutive 1° oscillation images was recorded with a Mar300 CCD detector at a crystal-to-detector distance of 180 mm for refinement data and 150 mm for phasing data separately, with an exposure of 2 s per image. Data reduction was carried out with the HKL2000 suite¹¹ (Table I). Initial phases were calculated by the Ca-SAS method with the program SOLVE/RESOLVE^{12,13} incor-

porated in the high throughput structure determination pipeline Sca2Structure.¹⁴ Automated model building was carried out with ARP/wARP.¹⁵ Iterative model validation, rebuilding and refinement were carried out with MOLPROBITY,^{16,17} XFIT¹⁸ and the CCP4 program REFMAC5,¹⁹ respectively. ARP/wARP and CCP4 programs were controlled through the CCP4I interface.²⁰ The final refinement statistics are shown in Table I. Coordinates of the refined model were deposited in the Protein Data Bank (PDB)²¹ with access code 2HQ8.

Molecular docking

The model structure of *R. muelleri* luciferase was built using the three-dimensional structure of *R. reniformis* luciferase²² (PDB code 2PSD) as a template (Web-server ESyPred3D: <http://www.fundp.ac.be/sciences/biologie/urbm/bioinfo/esypred/>). This template shares 91.8% identity with the *R. muelleri* luciferase sequence. The molecular docking was carried out with the use of the PatchDock program²³ which algorithm is based on shape complementarity principles (Web-server: <http://bioinfo3d.cs.tau.ac.il/PatchDock/patchdock.html>). For the docking computation request, the default conditions were specified: 4 Å for the “Clustering RMSD” parameter, any type of configuration for the complex, and no specific residues indicated as possible interaction sites.

RESULTS AND DISCUSSION

Overall structure

Figure 1 demonstrates that the structure of the apo-CBP with three bound Ca²⁺ and lacking the coelenterazine in the binding cavity, has the same compact scaffold and characteristic two-domain fold as the CBP itself before the addition of Ca²⁺. In Figure 1(A) calcium atom is seen located in each of the canonical Ca²⁺-binding sites, EF-hand loops I, III, and IV. Although the two proteins share the same overall fold, there are easily discerned local structure differences in almost every part, both in the helical and the loop regions. The RMSD of the C α atoms between the two conformations is 3.91 Å. However, it should be noted that Ca²⁺ binding induces a greater conformational change in the N-terminal domain than at the C-terminus (Fig. 1, Table II).

Interactions between EF-hand motifs in N- and C-terminal domains

In the family of EF-hand proteins, the EF-hand motif almost always occurs in pairs. This double motif appears to be important for correct structural folding, and is thought to increase the affinity of each EF-hand for calcium.²⁴ Figure 2(A,C) shows that in CBP, the paired EF-hands display extensive hydrophobic interhelical inter-

actions and a short β -type interaction between the two binding loops.

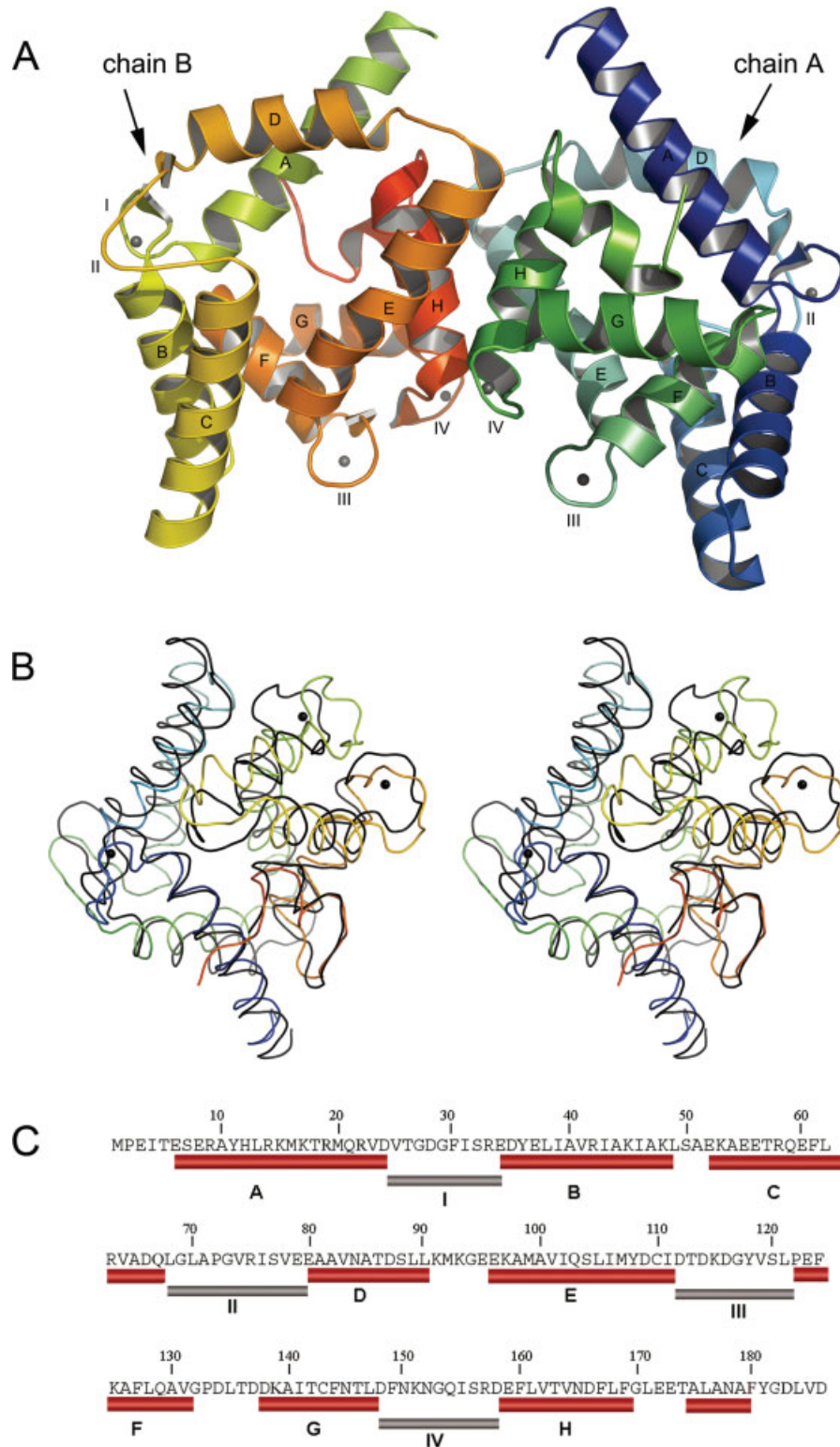
The EF-hand motif I of CBP is paired with EF-hand motif II, the latter having the characteristic structural features of an EF-hand motif but not the canonical sequence in the loop to permit calcium binding. The two loops of EF-hand motifs I and II also show typical interaction [Fig. 2(A)]. Loop I is bound with the loop II by means of hydrogen bonds between main chain nitrogen and carbonyl oxygen atoms of Ile31 and Ile76, main chain carbonyl oxygen and nitrogen atoms of Gly29 and Val78, the side chain O ^{δ 1} of Asp28 and the side chain nitrogen atom of Arg75, and between N ^{ϵ} of Arg33 and the main chain carbonyl oxygen atom of Leu70 [Fig. 2(A)]. In Ca²⁺-loaded apo-CBP [Fig. 2(B)], the hydrogen bond pattern of loop-loop interaction is practically the same; the binding of calcium ion abolishes only the hydrogen bond between the side chain O ^{δ 1} of Asp28 and the side chain nitrogen atom of Arg75.

The loops of EF-hand motifs III and IV interact with each other as well both in the Ca²⁺-free and in Ca²⁺-loaded states of CBP [Fig. 2(C,D)]. The interaction occurs through hydrogen bonds between main chain nitrogen and carbonyl oxygen atoms of Val119 and Ile155. These hydrogen bonds are found both in Ca²⁺-free and in Ca²⁺-loaded states of CBP. In the Ca²⁺-free state of CBP, there is a hydrogen bond between the main chain carbonyl oxygen atom of Gly117 and the main chain nitrogen of Arg157, which gets lost on binding of calcium ions into these loops.

Interhelical angles

The conformational changes that result from calcium binding to loops of the EF-hand motifs are usually described by the interhelical angles that represent more complex rearrangements of the interfaces between the α -helices of the domains.²⁵ Although such a description of Ca²⁺-induced conformational transients is available only for a few Ca²⁺-binding proteins, it provides a useful framework within which different types of conformational changes can be examined. For instance, the EF-hand motifs of “calcium-sensor class” proteins calmodulin and troponin C, are approximately anti-parallel in the Ca²⁺-free state, but they become nearly perpendicular in the Ca²⁺-loaded state.²⁵ This reorientation of α -helices exposes a hydrophobic patch, which is the basis of the biological function of these two proteins in living cells.

Unlike calmodulin or troponin C, the interhelical angles in CBP are almost perpendicular already in its Ca²⁺-free state and Ca²⁺ binding does not change these angles significantly (Table III). In comparison to the effects in calmodulin and troponin C, we can conclude that the α -helices of CBP are optimally oriented for calcium binding. Nevertheless the movements of these helices on Ca²⁺ binding although small (Table III), appear

**Figure 1**

A. The crystal structure of *R. muelleri* Ca^{2+} -loaded apo-CBP. The protein crystallized as a dimer (the chains are designated by arrows, helices are in multicolor). B. Stereoview of the superposition of *R. muelleri* CBP (the bound coelenterazine not included) (PDB code 2HPS, multicolor) and the Ca^{2+} -loaded apo-CBP (PDB code 2HQ8, black). Calcium ions are shown as the gray balls in both cases. C. Primary structure of CBP; red bars correspond to the helices and gray the EF-hand loops.

Table IIRMS Deviation Values of Ca²⁺-loaded apo-CBP versus CBP Bound with Coelenterazine

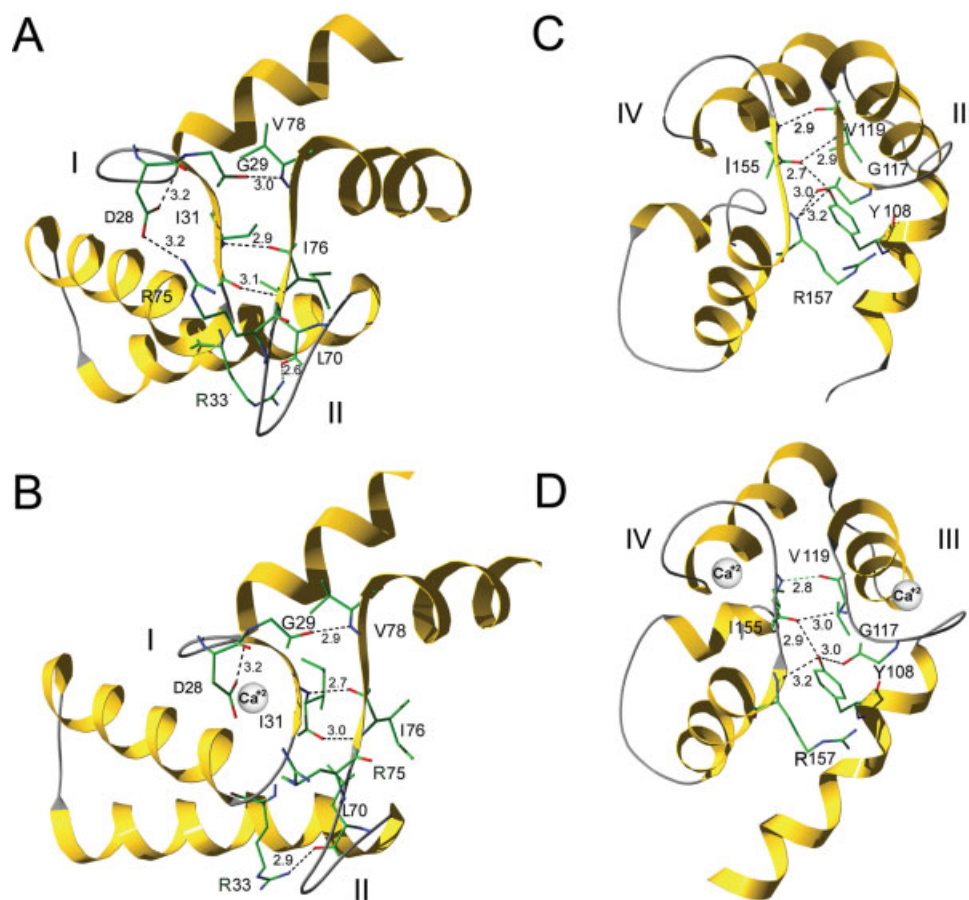
Structural parts of CBP	RMSD of C α atoms (Å)
Overall	3.91
N-terminal domain	3.09
C-terminal domain	1.83
Loop I	1.68
Loop II	2.16
Loop III	0.95
Loop IV	0.62

to be sufficient to reduce solvent exposure of the coelenterazine on one side of the structure but also to induce the formation of a “hole” on the other side, an “escape route” for the molecule. This is shown by the surface model (see Fig. 3) where the CBP has solvent exposure at the 6-(*p*-hydroxyphenyl) position that then closes up to

form the “escape hole” at the other end of the coelenterazine, at the 2-(*p*-hydroxybenzyl) substituent (see also Fig. 5). It is interesting that this region of the molecule is also the site of oxygen addition and it would seem very desirable that the luciferase should be nearby to efficiently capture coelenterazine before it would be lost through autooxidation.

Calcium-binding loops

Strynadka and James²⁴ proposed that conformational “pre-forming” of the ligands in a Ca²⁺-binding loop would decrease the energetic cost in ordering this site for optimal Ca²⁺ binding. Among the Ca²⁺-binding sites of CBP, the residues in Ca²⁺-binding loops III and IV are found to be in this pre-formed state; they have to adjust only a little to accommodate a calcium ion. The RMSD between Ca²⁺-loaded and Ca²⁺-free states of the residues of these loops are 0.95 and 0.62 Å, respectively (Table II).

**Figure 2**

Small shifts of helix interactions in CBP (A, C) on Ca²⁺ binding (B, D) are typical of EF-hand proteins of the “Ca²⁺-signal modulator” class.²⁵ A and B are the N-terminal EF-hands where one Ca²⁺ locates into loop I, and C and D are at the C-terminal with one Ca²⁺ binding to loops III and IV. The dashed lines are inferred H-bonds and numbers are Å separation of donor and acceptor.

Table III
Interhelical Angles and Distances^a

α -helices	Interhelical angle (CBP/Ca ²⁺ -loaded apo-CBP)	Interhelical distance ^b (CBP/Ca ²⁺ -loaded apo-CBP) (Å)
A–B	67.534/65.146	22.984/24.313
C–D	95.877/68.199	17.945/24.864
E–F	106.853/101.210	17.020/17.781
G–H	101.584/101.001	14.979/14.991

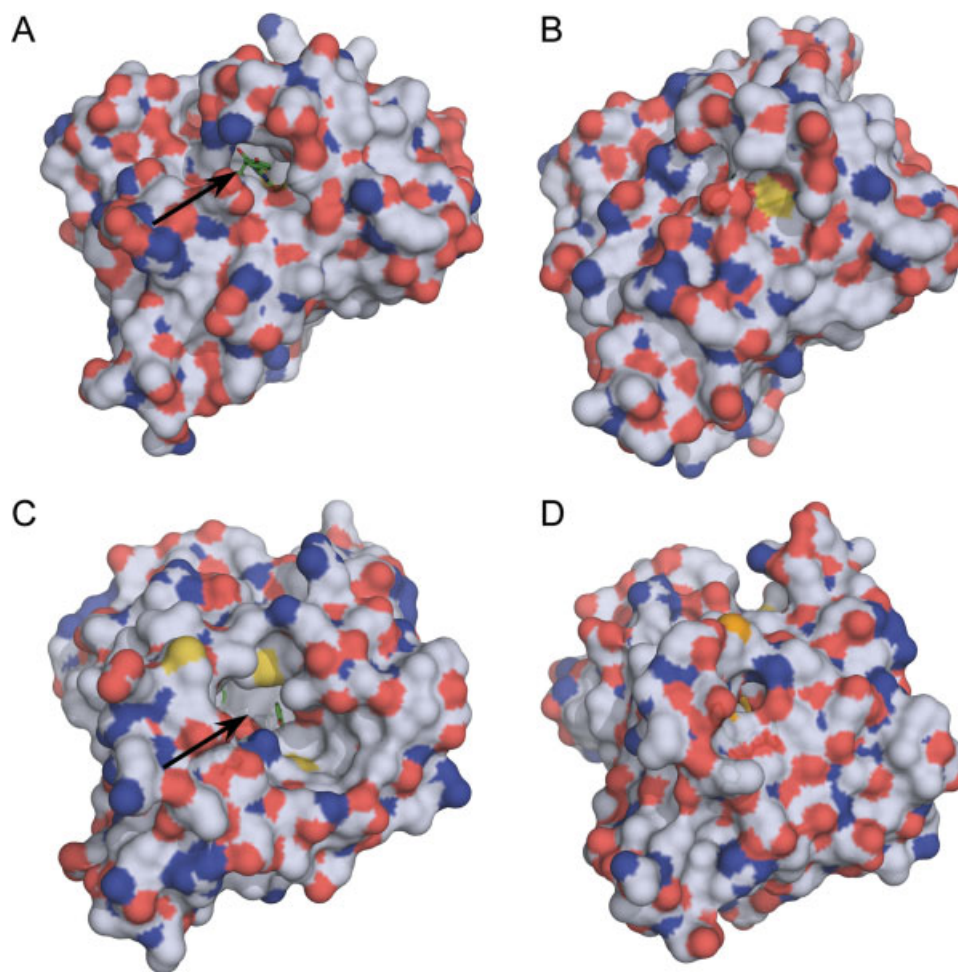
^aThe interhelical angles and distances were calculated using interhix (K. Yap, University of Toronto).

^bThe distance between midpoints of the corresponding α -helices.

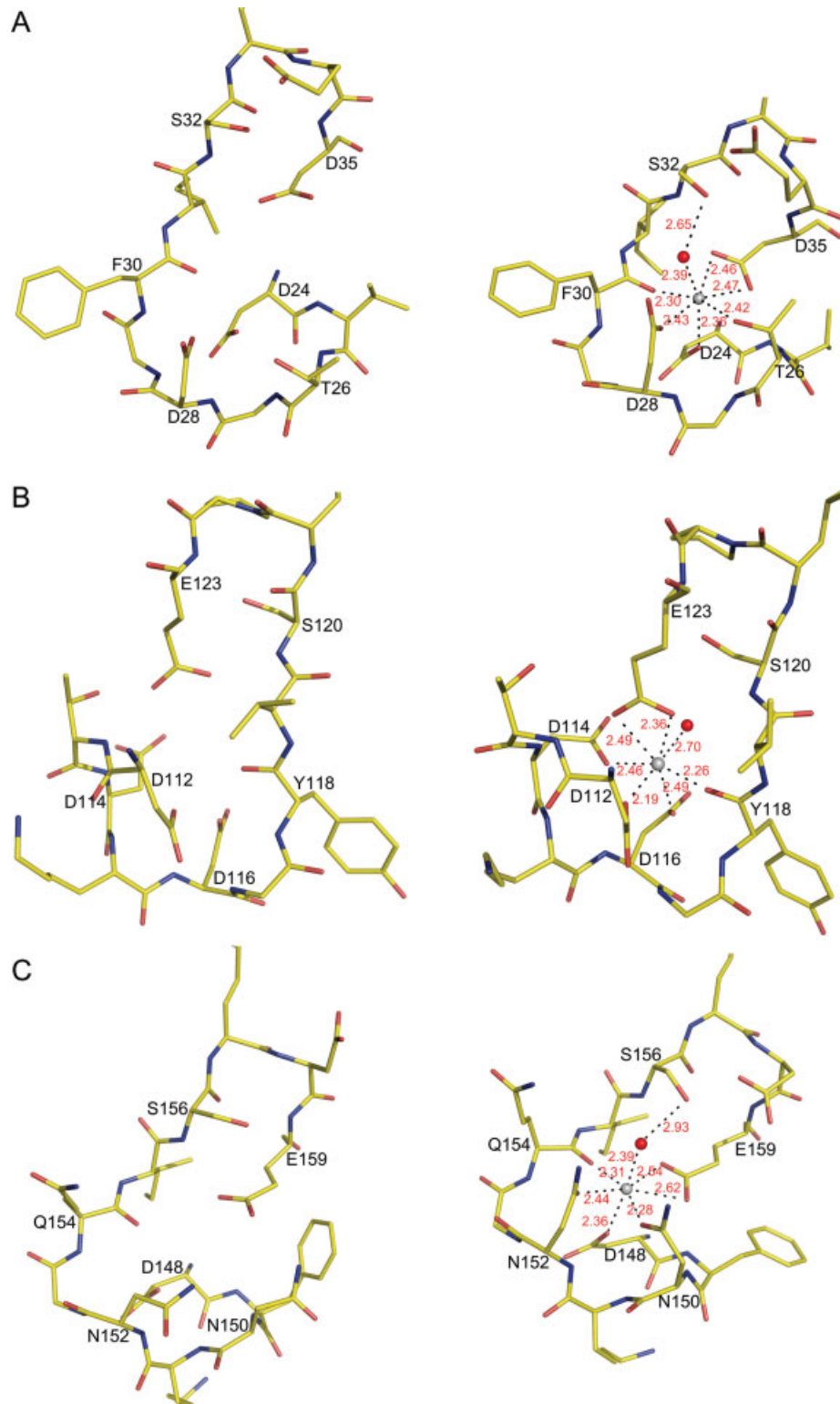
As a consequence, the Ca²⁺-binding loops III and IV should have a higher affinity for calcium than does Ca²⁺-binding loop I, for which the RMSD between

Ca²⁺-loaded and Ca²⁺-free states is 1.68 Å. This higher RMSD might be a result of the twelfth position in loop I [D35, Fig. 4(A)], being occupied by Asp instead of the invariant Glu, as in canonical Ca²⁺-binding consensus sequences. Also this Asp residue maintains a bidentate Ca²⁺ coordination, leading to a contraction of the loop. So far, among numerous EF-hand proteins, a similar substitution of Glu in the twelfth position to Asp is found only in sarcoplasmic Ca²⁺-binding proteins.²⁶

Figure 4 shows how the 12 residues of the EF-hand Ca²⁺-binding loops (I, III and IV) shift their positions when going to the Ca²⁺-loaded states. In all these loops, typical geometrical arrangement of the ligating oxygen atoms in a pentagonal bipyramid is observed, with the Ca²⁺ ion occupying the center of the pyramid. Also in each there are six oxygen ligands derived from the car-

**Figure 3**

Molecular surface representation of CBP in Ca²⁺-free and Ca²⁺-loaded states. **A.** CBP loaded with coelenterazine (the green stick model), which can be seen through a solvent exposed opening (arrow). **B.** apo-CBP loaded with Ca²⁺ in the same orientation as CBP in (A), to show that the opening has closed up. **C.** apo-CBP loaded with Ca²⁺ viewed from the other side of the structure shows a new “hole” (arrow) exposing the cavity. **D.** CBP loaded with coelenterazine in the same orientation as apo-CBP loaded with Ca²⁺ in (C), to show that this “hole” is lacking before Ca²⁺ binding. The coelenterazine molecule is not actually present in the apo-CBP structure, but is placed there for the purpose of superimposing the CBP and apo-CBP structures. The white color represents carbon atoms, blue - nitrogen, red - oxygen and yellow - sulfur.

**Figure 4**

Structure of the Ca²⁺-binding loops in the Ca²⁺-free (left; PDB code 2HPS) and Ca²⁺-loaded (right; PDB code 2HQ8) states. A, B, and C are the Ca²⁺-binding loops I, III, and IV respectively. Calcium ions and water molecules are shown as gray and red balls, respectively. Distances are in Å. Ca²⁺-binding loops in the Ca²⁺-free and Ca²⁺-loaded states are shown in the same orientation.

boxylic side-chain of aspartate and glutamate residues and from carbonyl groups of the peptide backbone or the side-chain of asparagine, all with a bond-length to the metal ion around 2.4 Å (see Fig. 4). A seventh ligand comes from the oxygen atom of a water molecule in turn hydrogen bonded to a serine in position 9, for loops I and IV. This last hydrogen bond is absent in loop III [Fig. 4(B)]. These are typical configurations for proteins of the EF-hand super family except that the lack of a hydrogen bond between a coordinating water and the residue in position 9, is not a frequent occurrence.²⁴ A generalization is that proteins of this family having high affinity Ca²⁺-binding sites, have either no water or at most one water ligand. Since the each of the three Ca²⁺-binding sites of apo-CBP contain only one water molecule, they all should have a high affinity for the Ca²⁺. However, only two high affinity Ca²⁺-binding sites were observed by titration experiments for native CBP (LBP) of *R. reniformis*.³ These comparisons show that Ca²⁺-binding loop I undergoes the largest change in conformation, then loop IV, and those residues forming loop III hardly shift on the Ca²⁺ ligation, perhaps the explanation for the lack of interaction in loop III between the Ser120 and the coordinating water.

Coelenterazine-binding cavity

Figure 5(A) is a magnified view of the cavity part of the structure and shows that several residues adjacent to loop I are also repositioned as a result of the Ca²⁺ binding there. Some of these comprise the binding cavity and interact directly with the bound coelenterazine in CBP.⁸ Interestingly, the Arg19-Tyr36 forms a “lid” over the coelenterazine-binding cavity, which becomes opened up in the Ca²⁺-loaded structure.

Figure 5(B) is a two dimensional picture to show more clearly the residue side-chain interactions that bind the coelenterazine in the CBP cavity and the shifts induced by Ca²⁺ binding. In addition to these shifts there is a slight decrease in cavity volume, 1044–960 Å³, and a change of shape. The C-terminus part of the cavity caves in, the N-terminus domain is slightly opened up and helices C, D and E move opposite each other to form a new solvent exposed broad area (see Fig. 3). The mechanism by which the coelenterazine dissociates becomes clear from this 2D diagram and is supported by structural modeling using appropriate software and the available PDB files. The strongly interacting residues in the CBP cavity are seen to have moved away such that one cannot place a model structure in any position so that the original hydrogen bonds, specifically those to the waters, W₁–W₅, can reform. Thus, the interactions are weakened and the coelenterazine escapes through the opened Arg19 lid and “hole” formed by helices C, D, and E.

The conformational changes around the cavity can be examined in detail from the PDB files. The Arg22 side

Table IV

Molecular Docking Computation^a of *Renilla* luciferase to the Ca²⁺-Loaded apo-CBP

Solution No.	Score	Area	ACE
1	13,140	1665.80	213.93
2	12,100	1557.60	374.56
3	11,916	1617.00	93.12
4	11,688	1614.50	104.40
5	11,658	1470.30	376.48
6	11,626	1461.90	388.49
7	11,480	1492.00	350.31
8	11,390	1551.20	249.01
9	11,294	1361.20	327.86
10	11,284	1494.30	25.71
15	10,942	1386.30	–58.37
16	10,874	1719.20	494.76
17	10,836	1528.30	438.88
18	10,804	1555.50	456.17
19	10,784	1361.20	416.36
20	10,732	1685.90	449.93

The top 20 solutions based on the shape complementary principle are listed. The first column is the geometric shape complementarity score, the next is the area of interaction, and ACE is the desolvation energy.

^aRef. 23.

chain bends and moves away along with its three water molecules, from its original position that formed a cap over the coelenterazine C3-oxygen. Interactions at the original 2-(*p*-hydroxybenzyl) of coelenterazine are lost. The Tyr36 benzyl ring is rotated 90°, the Gln103 side chain is turned over 180°, and the Arg19 side chain is moved slightly up towards the outside of the cavity [Fig. 5(B)]. Lys139 and Asp183, which indirectly coordinated the 6-(*p*-hydroxyphenyl) of coelenterazine via W₁ and W₂ come close together but still remain H-bonded to the two water molecules, although with some shift of the H-bond donor atom. Last but not least in significance, is the shift of Phe180, as this interaction was proposed in our previous article⁸ as affecting the pK of this N(7) thus inhibiting formation of the anion species there, the one required for the oxygen addition reaction. In addition to these residues, which directly participated in coelenterazine binding, there are major changes in a pool of hydrophobic side chains like Phe, Met, Val, Leu, that were contributing hydrophobicity in the CBP cavity. These Ca²⁺-induced conformational shifts taken together, simply explain the loss of affinity of the cavity for coelenterazine, whereby this substrate becomes readily available for the bioluminescence reaction with luciferase.

Docking computation

Table IV is an abbreviation of the PatchDoc output file, listing the top 20 docking solutions for a putative *Renilla* luciferase complex with Ca²⁺-loaded apo-CBP. They are arranged by geometric shape complementarity score and the first solution in a row with highest score

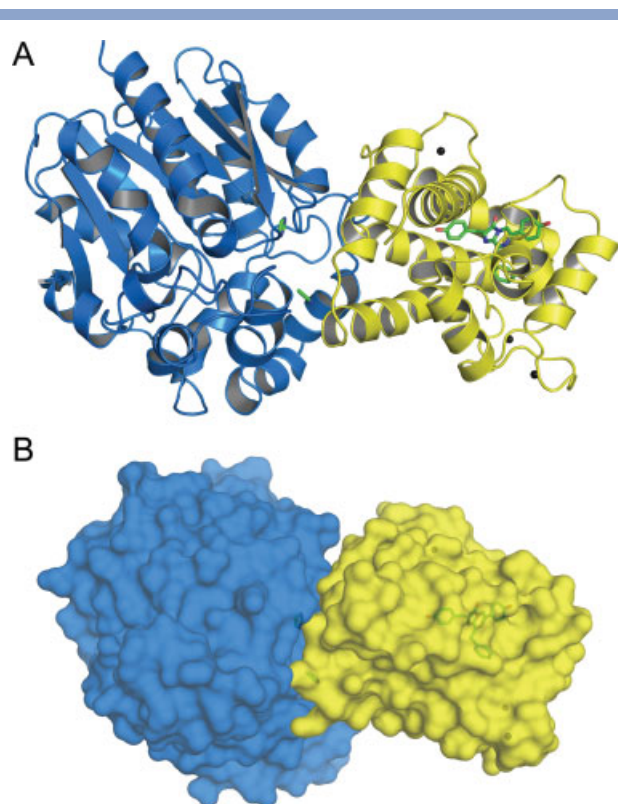


Figure 6

Computational docking of *R. muelleri* luciferase (blue) to the Ca^{2+} -loaded apo-CBP (yellow). **A** and **B** are the ribbon and molecular surface representations of the computational solution 1 from Table IV. The coelenterazine molecule is not actually present in the apo-CBP structure, but is placed there for the purpose of superimposing the CBP and apo-CBP structures. Black balls show calcium ions in apo-CBP; green pentagons show the two imidazole molecules observed in the *Renilla* luciferase structure (PDB 2PSD).

and largest interface area of interaction of the two proteins, is displayed in Fig. 6.

The authors of PatchDoc point out that a “near-native result is found among the top 100, and very often among the top 10 solutions” so it is interesting to find here that the model in Figure 6 places the “opened hole” in Ca^{2+} -apo-CBP, formed by helices C, D, and E and through which we propose the coelenterazine might escape, opposite the *Renilla* luciferase active site, the location of which has to be inferred from the position of two imidazole molecules that are known inhibitors.²² Allowing caution in interpreting this computational solution, at least the result gives some credence to the idea that the bioluminescent reaction might occur in a luciferase-CBP complex.

ACKNOWLEDGMENTS

Crystallographic data were collected at the Southeast Regional Collaborative Access Team (SER-CAT) 22-ID

beamline at the Advanced Photon Source, Argonne National Laboratory. Supporting institutions may be found at www.ser-cat.org/members.html.

REFERENCES

- Daunert S, Deo SK, editors. Photoproteins in bioanalysis. Weinheim: Wiley-VCH; 2006. 240 p.
- Matthews JC, Hori K, Cormier MJ. Purification and properties of *Renilla reniformis* luciferase. *Biochemistry* 1977;16:85–91.
- Charbonneau H, Cormier MJ. Ca^{2+} -induced bioluminescence in *Renilla reniformis*. Purification and characterization of calcium-triggered luciferin-binding protein. *J Biol Chem* 1979;254:769–780.
- Ward WW, Cormier MJ. An energy transfer protein in coelenterate bioluminescence. Characterization of the *Renilla* green fluorescent protein. *J Biol Chem* 1979;254:781–788.
- Hastings JW, Dunlap JC. Cell-free components in dinoflagellate bioluminescence. The particulate activity: scintillons; the soluble components: luciferase; luciferin, and luciferin-binding protein. *Methods Enzymol* 1986;133:307–327.
- Kumar S, Harrylock M, Walsh KA, Cormier MJ, Charbonneau H. Amino acid sequence of the Ca^{2+} -triggered luciferin binding protein of *Renilla reniformis*. *FEBS Lett* 1990;268:287–290.
- Titushin MS, Markova SV, Frank LA, Malikova NP, Stepanyuk GA, Lee J, Vysotski ES. Coelenterazine-binding protein of *Renilla muelleri*: cDNA cloning, overexpression, and characterization as a substrate of luciferase. *Photochem Photobiol Sci* 2008;7:189–196.
- Stepanyuk GA, Liu ZJ, Markova SV, Frank LA, Lee J, Vysotski ES, Wang BC. Crystal structure of coelenterazine-binding protein from *Renilla muelleri* at 1.72 Å: why it is not a calcium-regulated photoprotein. *Photochem Photobiol Sci* 2008;7:442–447.
- Vysotski ES, Liu ZJ, Rose J, Wang BC, Lee J. Preparation and X-ray crystallographic analysis of recombinant obelin crystals diffracting to beyond 1.1 Å. *Acta Crystallogr D Biol Crystallogr* 2001;57:1919–1921.
- Liu ZJ, Tempel W, Ng JD, Lin D, Shah AK, Chen L, Horanyi PS, Habel JE, Kataeva IA, Xu H, Yang H, Chang JC, Huang L, Chang SH, Zhou W, Lee D, Praissman JL, Zhang H, Newton MG, Rose JP, Richardson DC, Wang BC. The high-throughput protein-to-structure pipeline at SECSG. *Acta Crystallogr D Biol Crystallogr* 2005; 61:679–684.
- Otwinowski Z, Minor W. Processing of X-ray diffraction data collected in oscillation mode. *Methods Enzymol* 1997;276:307–326.
- Terwilliger TC. SOLVE and RESOLVE: automated structure solution and density modification. *Methods Enzymol* 2003;374:22–37.
- Terwilliger TC, Berendzen J. Automated MAD and MIR structure solution. *Acta Crystallogr D Biol Crystallogr* 1999;55:849–861.
- Liu ZJ, Lin D, Tempel W, Praissman JL, Rose JP, Wang BC. Parameter-space screening: a powerful tool for high-throughput crystal structure determination. *Acta Crystallogr D Biol Crystallogr* 2005; 61:520–527.
- Perrakis A, Harkiolaki M, Wilson KS, Lamzin VS. ARP/wARP and molecular replacement. *Acta Crystallogr D Biol Crystallogr* 2001;57: 1445–1450.
- Davis IW, Murray LW, Richardson JS, Richardson DC. MOLPROBITY: structure validation and all-atom contact analysis for nucleic acids and their complexes. *Nucleic Acids Res* 2004;32 (Web Server issue):W615–W619.
- Arendall WB, III, Tempel W, Richardson JS, Zhou W, Wang S, Davis IW, Liu ZJ, Rose JP, Carson WM, Luo M, Richardson DC, Wang BC. A test of enhancing model accuracy in high-throughput crystallography. *J Struct Funct Genomics* 2005;6:1–11.

18. McRee DE. XtalView/Xfit—A versatile program for manipulating atomic coordinates and electron density. *J Struct Biol* 1999;125:56–65.
19. Winn MD, Murshudov GN, Papiz MZ. Macromolecular TLS refinement in REFMAC at moderate resolutions. *Methods Enzymol* 2003;374:300–321.
20. Potterton E, Briggs P, Turkenburg M, Dodson E. A graphical user interface to the CCP4 program suite. *Acta Crystallogr D Biol Crystallogr* 2003;59:1131–1137.
21. Berman HM, Westbrook J, Feng Z, Gilliland G, Bhat TN, Weissig H, Shindyalov IN, Bourne PE. The Protein Data Bank. *Nucleic Acids Res* 2000;28:235–242.
22. Loening AM, Fenn TD, Gambhir SS. Crystal structures of the luciferase and green fluorescent protein from *Renilla reniformis*. *J Mol Biol* 2007;374:1017–1028.
23. Schneidman-Duhovny D, Inbar Y, Nussinov R, Wolfson HJ. PatchDock and SymmDock: servers for rigid and symmetric docking. *Nucleic Acids Res* 2005;33(Web Server issue):W363–W67.
24. Strynadka NC, James MN. Crystal structures of the helix-loop-helix calcium-binding proteins. *Annu Rev Biochem* 1989;58:951–998.
25. Nelson MR, Chazin WJ. Structures of EF-hand Ca²⁺-binding proteins: diversity in the organization, packing and response to Ca²⁺ binding. *Biometals* 1998;11:297–318.
26. Cook WJ, Ealick SE, Babu YS, Cox JA, Vijay-Kumar S. Three-dimensional structure of a sarcoplasmic calcium-binding protein from *Nereis diversicolor*. *J Biol Chem* 1991;266:652–656.